Molecular spectroscopy from 5-12 μm using an OP-GaP OPO

Molecular spectroscopy from 5-12 µm using an OP-GaP OPO

Luke Maidment[a], Peter G. Schunemann[b], Derryck T. Reid*[a]
[a]Scottish Universities Physics Alliance (SUPA), Institute of Photonics and Quantum Sciences, School of Engineering and Physical Sciences, Heriot–Watt University, Edinburgh EH14 4AS, UK;
[b]BAE Systems, Inc., MER15-1813, P.O. Box 868, Nashua, NH, USA 03061-0868

ABSTRACT

We report a femtosecond optical parametric oscillator (OPO) based on the new semiconductor gain material orientation patterned gallium phosphide (OP-GaP) and being the first example of a broadband OPO operating across the molecular fingerprint region. OP-GaP crystals with lengths of 1 mm and several patterning periods were diced, polished, and anti-reflection (AR) coated for near- to mid-infrared wavelengths. We configured a synchronously pumped OP-GaP OPO in a 101.2-MHz resonator with high reflectivity from 1.15–1.35 µm, pumped with 150-fs pulses from a 1040-nm femtosecond laser (Chromacity Spark). The coating of one spherical mirror was optimized for transmission at the pump wavelength of 1040 nm and for high reflectivity at the resonant signal wavelength in a range from 1.15–1.35 µm, while the other spherical mirror collimated the idler beam emerging from the OP-GaP crystal and was silver coated to provide high reflectivity for all idler wavelengths. This collimated idler beam was output-coupled from the cavity by transmission through a plane mirror coated with high transmission for the idler wavelengths (5–12 µm) and high reflectivity for the signal wavelengths (1.15–1.35 µm) on an infrared-transparent ZnSe substrate. Idler spectra centered from 5.4–11.8 µm and extending to 12.5 µm were collected. The maximum average power was 55 mW at 5.4 µm with 7.5 mW being recorded at 11.8 µm. Details of Fourier transform spectroscopy using water vapor and a polystyrene reference standard are presented.

Keywords: OPGaP, gallium phosphate, OPO, optical parametric oscillator, fingerprint, spectroscopy, femtosecond.

1. INTRODUCTION

The spectral fingerprint region, which is loosely defined as spanning from 3–20-µm, is known to contain strong and characteristic absorption bands which can be used to identify chemicals from their ro-vibrational spectra, especially in the 8–12-µm band where molecular-bond absorption features are dense and unique. Fourier transform spectroscopy has until now been the prevailing paradigm, with black-body thermal sources being the only option for reaching these wavelengths. Thermal sources (typically globars) have major drawbacks, including their very limited beam quality and poor spectral and spatial brightness. In contrast, broadband coherent sources offer exciting new possibilities for molecular spectroscopy. Their temporal coherence is makes it possible to generate mid-infrared frequency combs [1,2], with applications in dual-comb spectroscopy [3–5], while their spatial coherence promises diffraction-limited focusing for applications such as free-space propagation for stand-off chemical detection [7] and near-field micro-spectroscopy [6].

When looking to replace thermal sources with a coherent alternative, ultrafast oscillators are immediately appealing because of their broad instantaneous bandwidth, which permits the gold-standard methodology of Fourier-transform spectroscopy (FTS) to continue to be applicable. In this way, the wavelength calibration is transferred from the source to the detection system [8] and the many advantages of FTS over grating-based spectroscopy can be realized, such as its excellent signal:noise characteristics and its wavelength-independent spectral resolution [9].

Current technical routes to broadband mid-infrared generation in the spectral fingerprint region include supercontinuum generation in chalcogenide fiber [10], synchrotrons [11,12], difference-frequency mixing between two near-infrared lasers [13] or different spectral components of broadband near-infrared pulses [14], and cascaded OPOs [15]. For different reasons, each of these approaches faces challenges associated with their complexity, low repetition rate, size or poor efficiency, limiting their potential for widespread adoption.

By contrast, femtosecond OPOs offer a compelling route to accessing the fingerprint region. In this paper we describe a very promising embodiment based on the new gain material orientation patterned gallium phosphate (OP-GaP), and the application of this system to some demonstration spectroscopy experiments.

2. ORIENTATION-PATTERNED GALLIUM PHOSPHATE

2.1 Candidate materials for femtosecond OPOs in the long-wave infrared generation

Over the past two decades, quasi-phasematched oxide materials, predominantly periodically-poled $LiNbO_3$ (PPLN) and periodically-poled $KTiOPO_4$ (PPKTP), have become the materials of choice for short- to mid-wave infrared generation. However, these materials suffer severe absorption above 5 μm and so must be ruled out for applications requiring access to the most useful spectroscopic 8–12-μm wavelength band. Semiconductor materials typically provide transparency much deeper into mid-IR, with demonstrations to date employing orientation-patterned gallium arsenide (OP-GaAs) being the most promising [16], addressing 4–14 μm with nanosecond pulses [15]. Femtosecond OPO pumping is limited by two-photon absorption (TPA) of the pump wavelength, which in turn constrains the choice of pump sources to those with suitable wavelength and pulse characteristics. In the case of OP-GaAs, two-photon absorption prevents it from being pumped at wavelengths below 1.7 μm, so its implementation in a femtosecond oscillator has been limited by the availability of suitable pump lasers to the production of idler wavelengths shorter than the fingerprint band [17].

In Table 1 several candidate quasi-phasematched materials for mid-infrared OPOs are compared. The attractions of OP-GaP are immediately obvious on account of its high nonlinearity, absence of problematic TPA and wide transparency.

Table 1. Comparison of common quasi-phasematched gain media for the mid-infrared region.

	OP-GaAs	OP-GaP	OP-ZnSe	PPLN	PPKTP
Nonlinearity d_{eff} (pm V^{-1})	$2/\pi \times 94$ [18]	$2/\pi \times 70.6$ [20]	$2/\pi \times 43$ [22,23]	$2/\pi \times 27.2$ [25]	$2/\pi \times 14.9$ [27]
Transparency (μm)	0.95 – 17 [19]	0.6 – 12 [21]	0.5 – 22 [24]	0.33 – 5.5 [26]	0.35 – 4.5 [28]
Comment	TPA below 1.7 μm	Pumpable at 1 μm	Immature QPM	Transparency limit	Transparency limit

2.2 Orientation-patterned gallium phosphide

The development of orientation-patterned gallium phosphide (OP-GaP) [20], represents the first new orientation-patterned semiconductor to produce meaningful output powers in nearly 15 years [29] and offers a new route to long-wave mid-infrared generation. OP-GaP improves on OP-GaAs in one important respect: its band edge lies in the visible region, so TPA above 1 μm is negligible, enabling it to be directly pumped with powerful 1-μm Yb-fiber lasers. Unlike other candidate materials, OP-GaP can be produced in high quality wafers and provides transparency extending to 12 μm, thus delivering excellent coverage of the spectroscopic fingerprint region. In many respects, OP-GaP therefore provides a natural extension to PPLN OPOs, which have shown excellent performance with 1-μm pumping.

In Fig. 1 we illustrate the relative coverage of PPLN and OP-GaP, alongside the mid-infrared absorption spectra of selected chemicals (methane, VX, sulfur mustard and sarin). It is particularly clear from these spectra that while the 3–5-μm region can offer some hope of detection of certain chemicals, they can only be reliably distinguished by observing their absorption features across a much wider wavelength range, and in particular in the band extending from 5–15 μm. Indeed, this is the motivation for the development of broadband OP-GaP OPO devices for chemical sensing and spectroscopy.

Figure 2 depicts the phasematching efficiency map for a 1-mm-long OP-GaP crystal, along with the transmission spectrum of OP-GaP. The wavevector mismatch $\Delta k = k_{pump} - k_{signal} - k_{idler} - 2\pi/\Lambda$ was calculated over a matrix of grating periods (Λ) and signal / idler wavelengths and used to obtain the phasematching efficiency factor $\mathrm{sinc}^2(\Delta kL/2)$, where L is the crystal length of 1 mm. From the data in Fig. 2 it can be seen that idler generation is possible throughout the OP-GaP transparency window by varying the quasi-phasematching period from 15–35 μm, values which are compatible with the capabilities of the hydride vapor phase epitaxy (HVPE) growth technique used to extend the thickness of the MBE-grown QPM layer to several hundred microns.

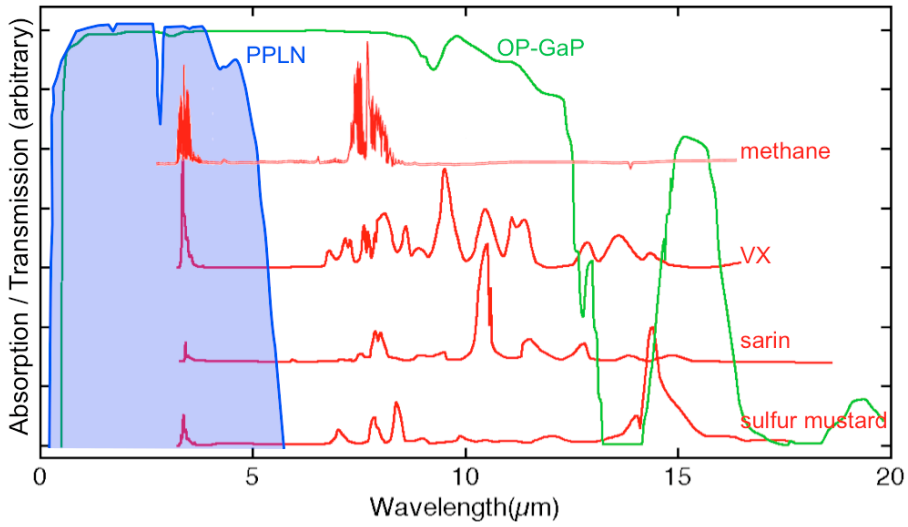

Fig. 1. OP-GaP and PPLN transmission coverage and their alignment with selected chemical absorption spectra.

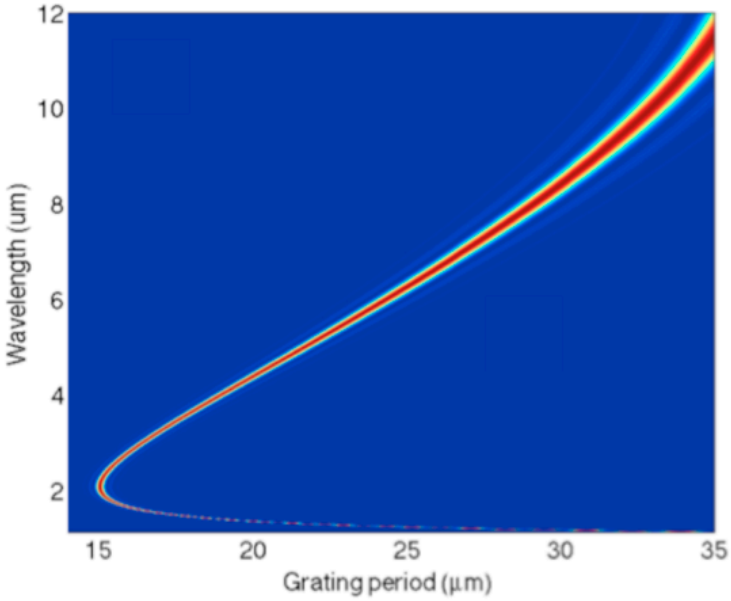

Fig. 2. Phasematching efficiency of OP-GaP for 1060-nm pumping and for a 1-mm-long crystal. Sellmeier data for the calculation are taken from Parsons *et al.*, Appl. Opt. **10**, 1683 (1971).

2.3 OP-GaP crystal fabrication

An OP-GaP wafer was prepared with eighteen distinct regions including patterning periods in the required range, as well as longer periods for evaluation purposes. The growth of this wafer has been described in detail already [30]. Figure 3 shows the layout of the wafer, and indicates the specific regions containing the shorter-period gratings relevant to 1-µm pumping.

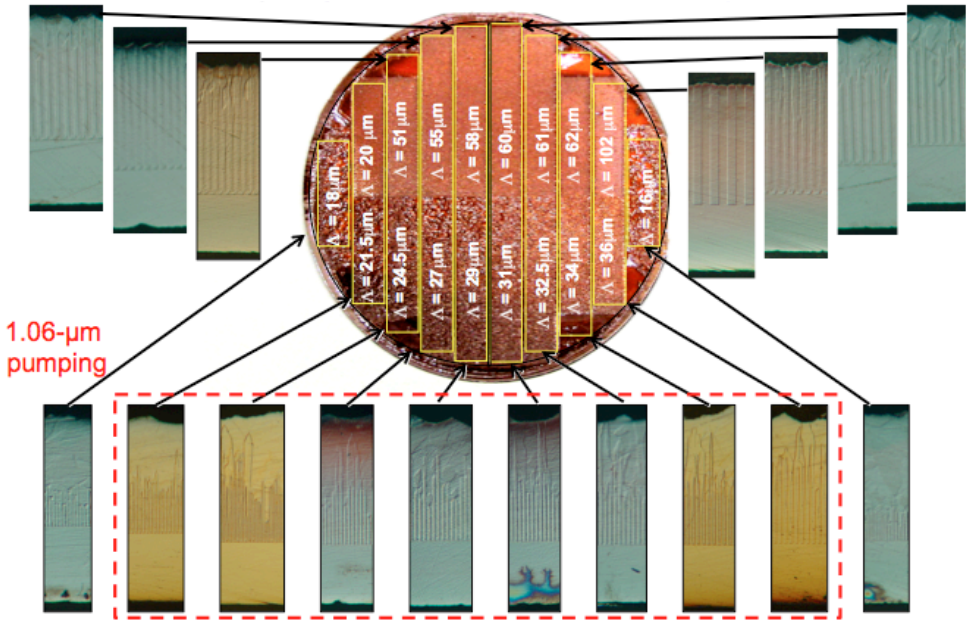

Fig. 3. Layout of the OP-GaP wafer (main image) and cross-sections through individual gratings (insets). The flat substrate can be seen in each inset, on top of which is grown a shallow MBE template followed by the extended grating structure grown by HVPE. The rough upper surface shows where HVPE growth ended. It can be seen that longer gratings can preserve the domain structure throughout the HVPE growth, while shorter gratings are observed to coalesce and lose fidelity further from the MBE template.

Operation at wavelengths > 5 μm and using 1-μm pumping requires seven OP-GaP crystals with domain periods from 21.5–34.0 μm. Despite the restricted aperture available due to domain coalescence, these grating periods remain perfectly usable.

3. SPECTROSCOPY USING AN OP-GAP FEMTOSECOND OPO

3.1 Configuration and performance of the OP-GaP femtosecond OPO

A schematic of the femtosecond OPO is shown in Fig. 4. The results discussed later were obtained using crystals with periods of 21.5, 24.5, 27.0, 29.0, 31.0, 32.5 and 34.0 μm, which were fabricated by the process described in [20]. The crystals were antireflection (AR) coated for 1.02 – 1.06 μm, 1.15 – 1.35 μm and 5 – 12 μm. The OPO was pumped by a 1040-nm Chromacity Spark femtosecond laser which was amplified to produce pulses with an average power of 2.7 W at a repetition rate of 100 MHz and a center wavelength of 1.04 μm. The pulses were compressed in a transmission-grating pulse compressor to < 200 fs. After loss from the pulse-compression and steering optics was accounted for, the beam power was 1.97 W. The pump was focused into a 1-mm OPGaP crystal configured as a signal-resonant ring cavity. The cavity optics had high reflectivity and low dispersion for the signal wavelengths from 1.15 – 1.35 μm, and high transmission for the pump (1.02 – 1.06 μm) and the idler (5 – 12 μm). The OPO cavity repetition rate was matched to the laser repetition rate for fundamental synchronous pumping. A 2% output coupler was used to extract the signal. The idler beam was extracted after reflection from an intracavity silver mirror and was transmitted through a plane ZnSe cavity mirror, following which an anti-reflection (AR) coated Ge window was used to remove the undepleted pump beam.

As can be seen in Fig. 5a, spectrally broad signal spectra were measured which were consistent with the phase matching calculations. By contrast, smooth and featureless idler spectra (Fig. 5b) were obtained, except where atmospheric water absorption introduced dense structure at wavelengths below 7 μm. For the OPGaP grating periods of 21.5, 24.5, 27, 29 and 31 μm, idler powers of 52, 23, 19, 13 and 10 mW respectively were measured. For Λ = 32.5 μm the output coupler was replaced with a plane high-reflectivity optic, resulting in 4 mW idler power.

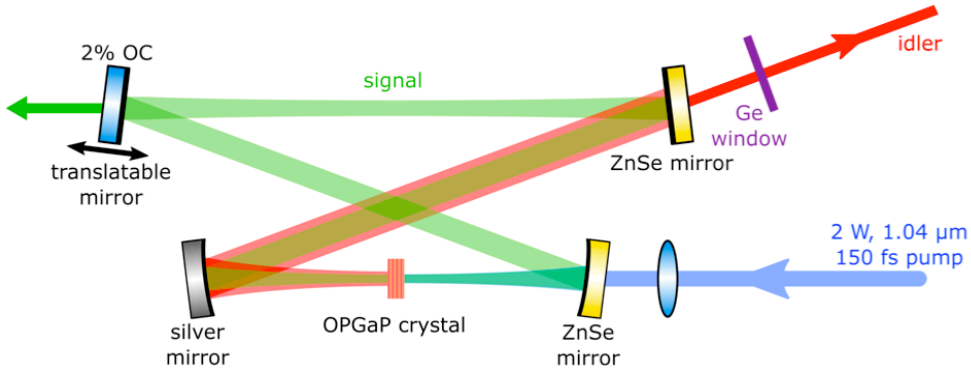

Fig. 4. Layout of the synchronously pumped OP-GaP ring OPO.

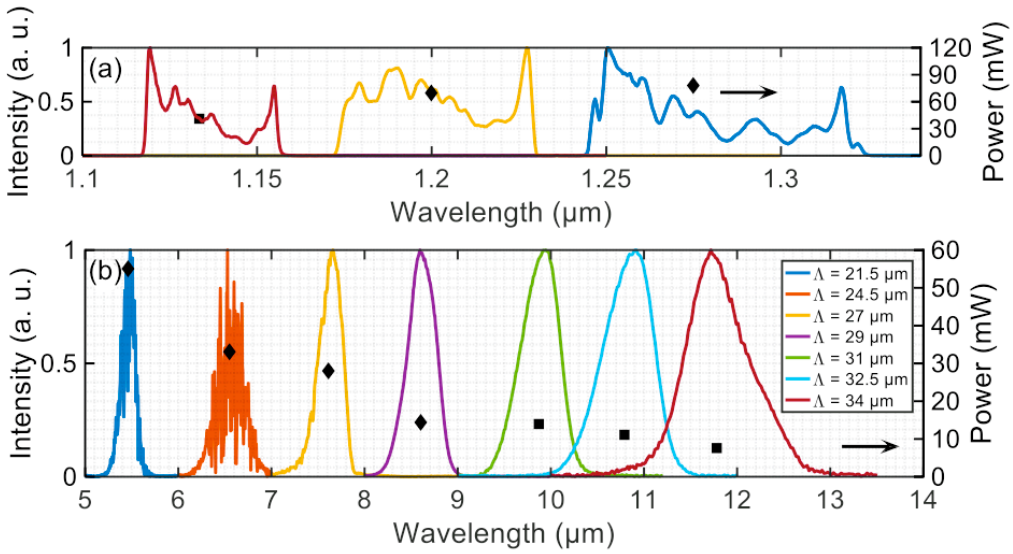

Fig. 5. (a) Selected signal spectra and (right axis) measured power. (b) Idler spectra and (right axis) measured power. Diamond markers represent measurements made using different cavity mirrors to the square markers.

3.2 Fourier-transform idler spectroscopy

Idler spectra centered from 5.4–11.8 μm and extending to 12.5 μm were collected (Fig. 5b) by steering the collimated idler beam to a scanning Michelson interferometer acting as a Fourier transform spectrometer. The maximum average power was 55 mW at 5.4 μm with 7.5 mW being recorded at 11.8 μm. The resulting interferogram was recorded using a mercury cadmium telluride (MCT) detector. Spectra for Λ = 21.5 and 24.5 μm (measured with 1.2 cm^{-1} resolution) showed significant structure due to the absorption by atmospheric water vapor in this wavelength region. Water vapor absorption is also visible on the short-wavelength side of the Λ = 27 μm spectrum.

We implemented a dual-detector Fourier-transform spectrometer to demonstrate the practicality of this source for molecular fingerprint-region spectroscopy. One detector was used to acquire a reference spectrum and the other to synchronously record the measurement spectrum. A polystyrene FTS reference sample normally used for calibration of commercial FTS instruments was used for the spectroscopy evaluation. By ratioing the spectrum transmitted through the polystyrene with the reference spectrum we accurately obtained the transmission profile of the sample while preventing any drift in the idler spectrum from influencing the measurement. At shorter wavelengths we used atmospheric water vapor absorption as our spectroscopy reference. Spectroscopy results are presented in Fig. 6, which includes the water vapor transmission spectra from the HITRAN molecular absorption database for comparison [31]. Excellent agreement

was obtained across the 5–13-µm region, representing a significant portion of the fingerprint region containing many of the diagnostic stretching and bending frequencies of important molecular functional groups.

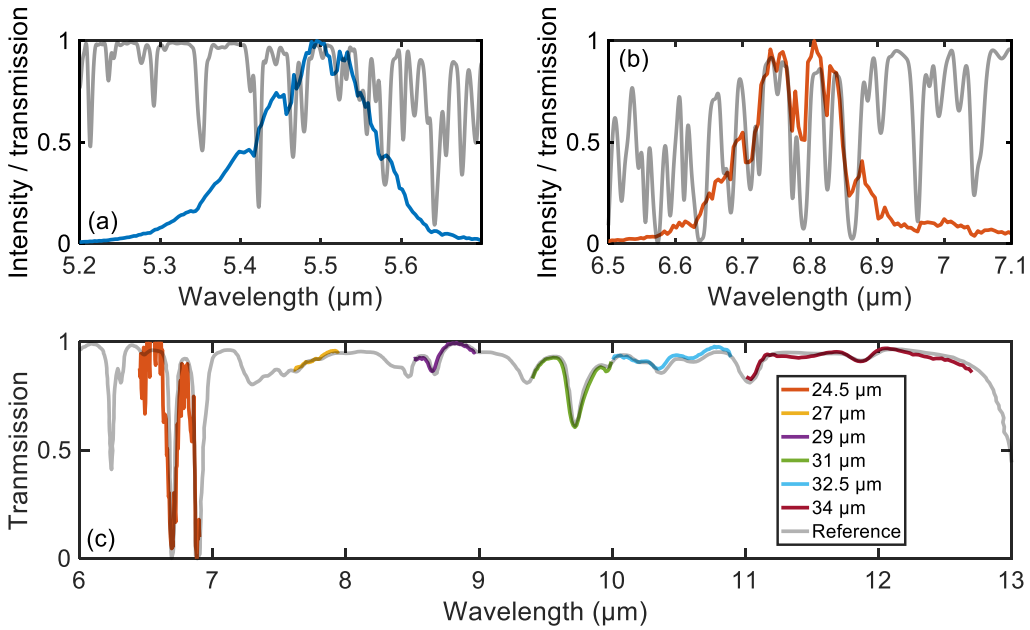

Fig. 6. Simulated water-vapor absorption spectra from the HITRAN database (grey) shown for comparison with idler spectra recorded from the OPO operated with OP-GaP grating periods of 21.5 µm (a) and 24.5 µm (b). (c) Transmission spectra of a polystyrene reference standard recorded from the OPO operated with OP-GaP grating periods of 24.5–34 µm and reference spectrum supplied by the sample manufacturer (grey).

4. CONCLUSIONS

OP-GaP allows the paradigm of coherent broadband Fourier-transform infrared spectroscopy to be extended into the spectroscopic fingerprint region. Access to this region, particularly at wavelengths > 5µm, was previously limited by the transparencies of oxide nonlinear media such as $LiNbO_3$, LiB_3O_5 and $KTiOPO_4$ or by the need to pump at wavelengths considerably greater than 1 µm to avoid two-photon absorption when using other semiconductor nonlinear gain media. These constraints are fully circumvented by the use of OP-GaP, which can therefore be expected to accelerate the development of new coherent spectroscopic applications of the mid-infrared in environmental sensing, security, healthcare, drug-quality screening, material science and optical histopathology.

ACKNOWLEDGMENTS

The authors are grateful to Chromacity Ltd. for the loan of a 1040-nm femtosecond pump laser.

REFERENCES

[1] A. Schliesser, N. Picqué, and T. W. Hänsch, "Mid-infrared frequency combs," Nature Photon 6, 440–449 (2012).
[2] K. Balskus, Z. Zhang, R. A. McCracken, and D. T. Reid, " Mid-infrared 333 MHz frequency comb continuously tunable from 1.95 to 4.0 µm," Opt. Lett. 40, 4178 (2015).
[3] B. Bernhardt, A. Ozawa, P. Jacquet, M. Jacquey, Y. Kobayashi, T. Udem, R. Holzwarth, G. Guelachvili, T. W. Hänsch, and N. Picqué, "Cavity-enhanced dual-comb spectroscopy," Nature Photon 4, 55–57 (2009).
[4] Z. Zhang, T. Gardiner, and D. T. Reid, "Mid-infrared dual-comb spectroscopy with an optical parametric oscillator," Opt. Lett. 38, 3148–3150 (2013).

[5] B. Bernhardt, E. Sorokin, P. Jacquet, R. Thon, T. Becker, I. T. Sorokina, N. Picqué, and T. W. Hänsch, " Mid-infrared dual-comb spectroscopy with 2.4 μm Cr2+:ZnSe femtosecond lasers," Appl. Phys. B Lasers Opt. 100, 3–8 (2010).
[6] P. Patoka, G. Ulrich, A. E. Nguyen, L. Bartels, P. A. Dowben, V. Turkowski, T. S. Rahman, P. Hermann, B. Kästner, G. Ulm, and E. Rühl, "Nanoscale plasmonic phenomena in CVD-grown MoS2 monolayer revealed by ultra-broadband synchrotron radiation based nano-FTIR spectroscopy and near-field microscopy," Opt. Express 24, 1154–1164 (2016).
[7] Z. Zhang, R. J. Clewes, C. R. Howle, and D. T. Reid, "Active FTIR-based stand-off spectroscopy using a femtosecond optical parametric oscillator," Opt. Lett. 39, 6005–8 (2014).
[8] J. Connes, " Recherches sur la spectroscopie par la transformation de Fourier.," Rev. Opt. Theor. Instrum. 40, (1961).
[9] P. B. Fellgett, "On the Ultimate Sensitivity and Practical Performance of Radiation Detectors," J. Opt. Soc. Am. 39, 970–976 (1949).
[10] C. R. Petersen, U. Møller, I. Kubat, B. Zhou, S. Dupont, J. Ramsay, T. Benson, S. Sujecki, N. Abdel-Moneim, Z. Tang, D. Furniss, A. Seddon, and O. Bang, "Mid-infrared supercontinuum covering the 1.4–13.3 μm molecular fingerprint region using ultra-high NA chalcogenide step-index fibre," Nature Photon 8, 830–834 (2014).
[11] W. D. Duncan and G. P. Williams, "Infrared synchrotron radiation from electron storage rings," Appl. Opt. 22, 2914–2923 (1983).
[12] P. Dumas and L. Miller, "The use of synchrotron infrared microspectroscopy in biological and biomedical investigations," Vib. Spectrosc. 32, 3–21 (2003).
[13] A. Sell, I. Pastirk, A. Brodschelm, R. Herda, T. Puppe, and A. Zach, " Approaches to generation of tunable mid-IR ultrafast pulses with fiber sources," Proc. SPIE 9467, 94672I (2015).
[14] I. Pupeza, D. Sánchez, J. Zhang, N. Lilienfein, M. Seidel, N. Karpowicz, I. Znakovskaya, M. Pescher, W. Schweinberger, V. Pervak, E. Fill, O. Pronin, Z. Wei, F. Krausz, A. Apolonski, and J. Biegert, " High-power sub-two-cycle mid-infrared pulses at 100 MHz repetition rate," Nature Photon 9, 721–724 (2015).
[15] K. L. Vodopyanov, I. Makasyuk, and P. G. Schunemann, "Grating tunable 4 - 14 μm GaAs optical parametric oscillator pumped at 3 μm," Opt. Express 22, 4131–4136 (2014).
[16] D. F. Bliss, C. Lynch, D. Weyburne, K. O'Hearn, and J. S. Bailey, "Epitaxial growth of thick GaAs on orientation-patterned wafers for nonlinear optical applications," J. Cryst. Growth 287, 673–678 (2006).
[17] W. C. Hurlbut, Y. S. Lee, K. L. Vodopyanov, P. S. Kuo, and M. M. Fejer, "Multiphoton absorption and nonlinear refraction of GaAs in the mid-infrared," Opt. Lett. 32, 668–670 (2007).
[18] T. Skauli, K. L. Vodopyanov, T. J. Pinguet, A. Schober, O. Levi, L. A. Eyres, M. M. Fejer, J. S. Harris, B. Gerard, L. Becouarn, E. Lallier, and G. Arisholm, "Measurement of the nonlinear coefficient of orientation-patterned GaAs and demonstration of highly efficient second-harmonic generation," Optics Letters 27, 628–630 (2002).
[19] Handbook of Optical Constants of Solids, ed. by E.D. Palik (Academic Press, Orlando,1985).
[20] L. A. Pomeranz, P. G. Schunemann, D. J. Magarrell, J. C. McCarthy, K. T. Zawilski, and D. E. Zelmon, "1-μm-pumped OPO based on orientation-patterned GaP," Proc. SPIE 9347, 93470K (2015).
[21] V. Tassev ; M. Snure ; R. Peterson ; K. L. Schepler ; R. Bedford ; M. Mann ; S. Vangala ; W. Goodhue ; A. Lin ; J. Harris ; M. Fejer ; Peter Schunemann, "Progress in orientation-patterned GaP for next-generation nonlinear optical devices," Proc. SPIE 8604, Nonlinear Frequency Generation and Conversion: Materials, Devices, and Applications XII, 86040V (March 12, 2013).
[22] Kanner GS, Marable ML, Singh NB, A. Berghmans, D. Kahler, and B. Wagner, A. Lin, M.M. Fejer, and J.S. Harris, K. L. Schepler, "Optical probes of orientation-patterned ZnSe quasi-phase-matched devices," Opt. Eng. 0001;48(11):114201-114201-5.
[23] H.P. Wagner, M. Kühnelt, W. Langbein, and J.M. Hvam, "Dispersion and second-order nonlinear susceptibility in ZnTe, ZnSe, and ZnS," Phys. Rev. B 58, 10494-10501 (1998).
[24] http://www.iiviinfrared.com/Optical-Materials/znse.html (accessed 5 January 2017)
[25] D.A.Roberts, "Simplified characterization of uniaxial and biaxial nonlinear optical crystals: a plea for standardization of nomenclature and conventions," IEEE J. Quant. Electr. 28(10), 2057–2074 (1992).
[26] R. L. Sutherland, Handbook of Nonlinear Optics (Marcel Dekker, New York, 1996), Chap. 3.
[27] A. Arie, G. Rosenman, V. Mahal, A. Skliar, M. Oron, M. Katz, and D.Eger, "Green and ultraviolet quasi-phase-matched second harmonic generation in bulk periodically-poled KTiOPO4," Opt. Commun.142, 265 (1997)
[28] D. Bierlein and H. Vanherzeele, "Potassium titanyl phosphate: properties and new applications," J. Opt. Soc. Am. B 6, 622 (1989).

[29] L. A. Eyres, P. J. Tourreau, T. J. Pinguet, C. B. Ebert, J. S. Harris, M. M. Fejer, B. Gerard, and E. Lallier, " Quasi-phasematched frequency conversion in thick all-epitaxial, orientation-patterned GaAs films," in Advanced Solid State Lasers, H. Injeyan, U. Keller, and C. Marshall, eds. (OSA, 2000), paper TuA2.

[30] Luke Maidment, Peter G. Schunemann, and Derryck T. Reid, "Molecular fingerprint-region spectroscopy from 5 to 12 μm using an orientation-patterned gallium phosphide optical parametric oscillator," Opt. Lett. 41, 4261-4264 (2016).

[31] L. S. Rothman, I. E. Gordon, Y. Babikov, A. Barbe, D. Chris Benner, P. F. Bernath, M. Birk, L. Bizzocchi, V. Boudon, L. R. Brown, A. Campargue, K. Chance, E. A. Cohen, L. H. Coudert, V. M. Devi, B. J. Drouin, A. Fayt, J. M. Flaud, R. R. Gamache, J. J. Harrison, J. M. Hartmann, C. Hill, J. T. Hodges, D. Jacquemart, A. Jolly, J. Lamouroux, R. J. Le Roy, G. Li, D. A. Long, O. M. Lyulin, C. J. Mackie, S. T. Massie, S. Mikhailenko, H. S. P. Muller, O. V. Naumenko, A. V. Nikitin, J. Orphal, V. Perevalov, A. Perrin, E. R. Polovtseva, C. Richard, M. A. H. Smith, E. Starikova, K. Sung, S. Tashkun, J. Tennyson, G. C. Toon, V. G. Tyuterev, and G. Wagner, "The HITRAN2012 molecular spectroscopic database," J. Quant. Spectrosc. Radiat. Transf. 130, 4–50 (2013).